

SUPPORTING INFORMATION
FOR
CHARACTERIZATION OF HALOGEN BONDED COMPLEXES IN SYSTEMS
WITH COMPETING HYDROGEN BONDING OR ELECTRON TRANSFER

A THESIS

SUBMITTED TO THE GRADUATE SCHOOL
IN PARTIAL FULFILLMENT OF THE REQUIREMENTS

FOR THE DEGREE

MASTERS OF SCIENCE

BY

EMMANUEL ADENIYI

DR. SERGIY ROSOKHA-ADVISOR

BALL STATE UNIVERSITY

MUNCIE INDIANA

JULY 2023

CONTENTS FIGURES

Figure S1. UV-Vis spectra of solutions containing CHI₃ and DMACN mixtures

Figure S2. UV-Vis spectra of solutions containing CHI₃ and DMABr mixtures

Figure S3. UV-Vis spectra of solutions containing CHI₃ and DMA mixtures

Figure S4. UV-Vis spectra of solutions containing CHI₃ and TEA mixtures

Figure S5. UV-Vis spectra of solutions containing CHI₃ and mMeODMA mixtures

Figure S6. UV-Vis spectra of solutions containing CHI₃ and pMeODMA mixtures

Figure S7. Benesi-Hildebrand plots based on the UV-Vis spectra of solutions of CHI₃ with amines 1:1.

Figure S8. Dependencies of the chemical shifts of the protons of CHI₃ on the concentration of trimethylamine (TEA), N,N-dimethylaniline (DMA), 4-(dimethylamino)benzotrile (DMABN), p-bromo-N,N-dimethylaniline (BrDMA) or 3-(N,N-dimethylamino)anisidine (MeODMA).

Figure S9. Dependencies of the chemical shifts of the protons of CHBr₃ on the concentration of TEA, DMA, DMABN, BrDMA and MeODMA.

Figure S10. Dependencies of the chemical shifts of the protons of CHCl₃ on the concentration of TEA, DMA, DMABN, BrDMA and MeODMA.

Figure S11. ¹HNMR shifts occurring upon the addition of pMeODMA to solutions containing CHI₃ (A), CHBr₃(B), and CHCl₃ (C).

Figure S12. ¹HNMR shifts occurring upon the addition of DMAF to solutions CHBr₃(A), and CHCl₃ (B).

Figure S13. Electrostatic potential (calculated at 0.001 electrons Bohr⁻³ electronic density) on the molecular surfaces of other aromatic amines.

Figure S14. Dependencies of the Δ Abs and $\Delta\delta$ values in the solutions with a constant concentration of CHI₃ (0.01 M) and variable aliphatic and aromatic amine concentrations. The solid lines show the simultaneous multivariable fitting of the UV-Vis and NMR titration data.

Figure S15. UV-Vis spectra of solutions containing H-Im-iPrArI and TBACl mixtures

Figure S16. UV-Vis spectra of solutions containing H-Im-iPrArH and TBABr mixtures

Figure S17. UV-Vis spectra of solutions containing I₂ and DMACN mixtures

Figure S18. UV-Vis spectra of solutions containing I₂ and DMAF mixtures

Figure S19. UV-Vis spectra of solutions containing I₂ and pMeODMA mixtures

Figure S20. UV-Vis spectra of solutions containing I₂ and MPTZ mixtures

Figure S21. Dependencies of the Δ Abs and $\Delta\delta$ values in the solutions with a constant concentration of I₂ and variable aliphatic and aromatic amine concentrations.

TABLES

Table S1: Energies of HyB and HaB complexes between CHX_3 and amines obtained from M06-2X/def-TZVPP computations (acetonitrile).

Table S2: Energies of individual CHX_3 and amines obtained from M06-2X/def-TZVPP computations (acetonitrile).

Table S3. Electron densities and energies ($\rho(r)$ and $H(r)$, in a.u.) at BCPs along HaB and HyB bond paths

Table S4. Energies and UV-Vis values of HyB and HaB complexes between (halo)imidazolium and halides

Table S5. Energies of HaB complexes between molecular iodine with amines and some heterocyclic compounds in DCM, Acetonitrile, and Vacuum.

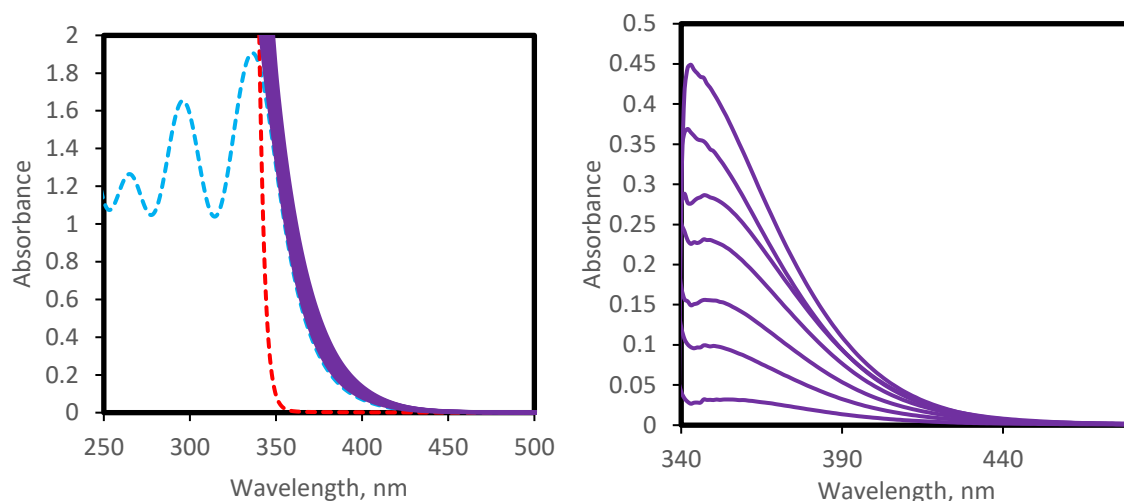


Figure S1. (Left) Spectra of the solutions with constant concentration of CHI_3 and various concentrations of p-cyano-N,N-dimethylaniline (DMACN). Spectra of the solutions of individual reactants are shown as dashed blue (CHI_3) or red (DMACN) lines. (Right): Spectra of the complexes obtained by subtraction of the absorption of components from the spectra of their mixtures.

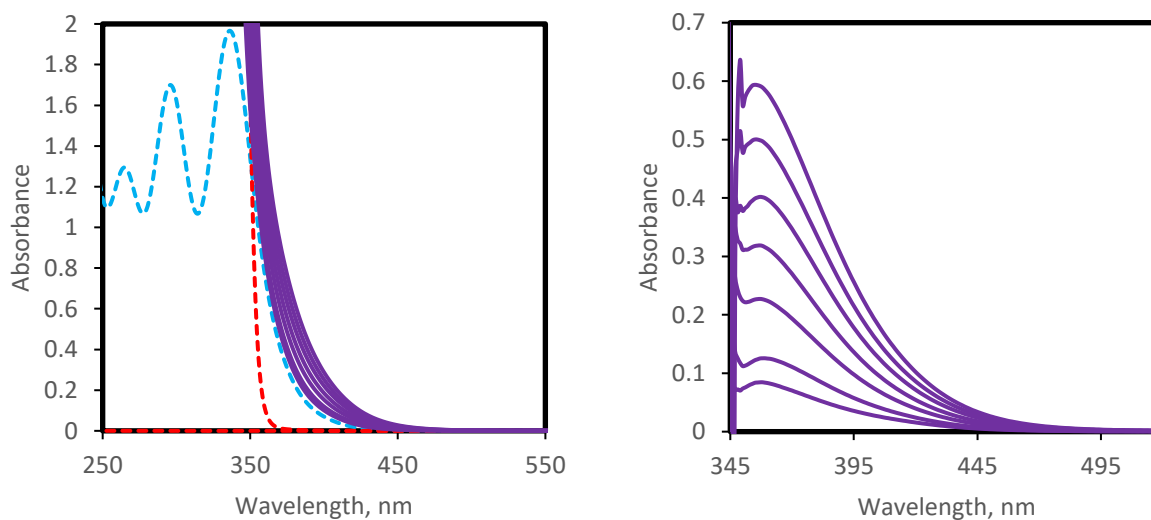


Figure S2. (Left) Spectra of the solutions with constant concentration of CHI_3 and various concentrations of p-bromo-N,N-dimethylaniline (DMABr). Spectra of the solutions of individual reactants are shown as dashed blue (CHI_3) or red (DMABr) lines. (Right): Spectra of the complexes obtained by subtraction of the absorption of components from the spectra of their mixtures

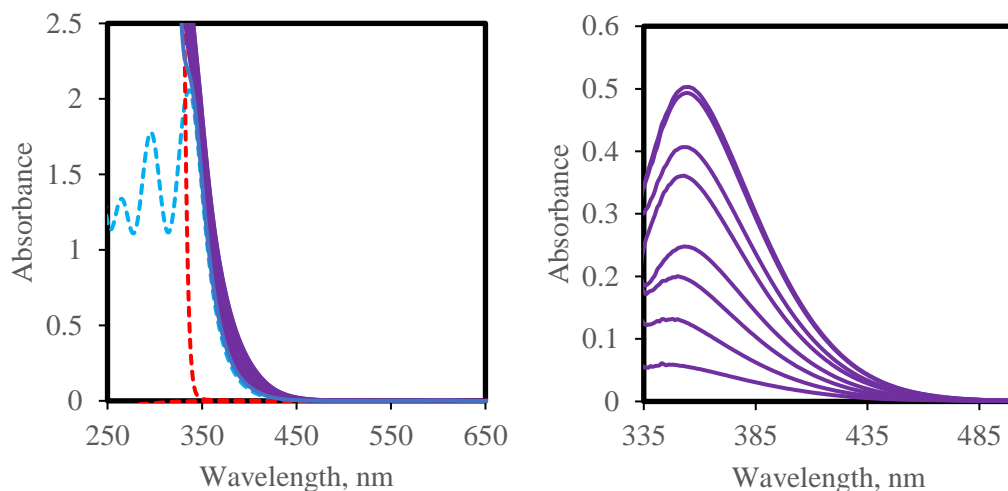


Figure S3. (Left) Spectra of the solutions with constant concentration of CHI_3 and various concentrations of N,N-dimethylaniline (DMA). Spectra of the solutions of individual reactants are shown as dashed blue (CHI_3) or red (DMA) lines. (Right): Spectra of the complexes obtained by subtraction of the absorption of components from the spectra of their mixtures

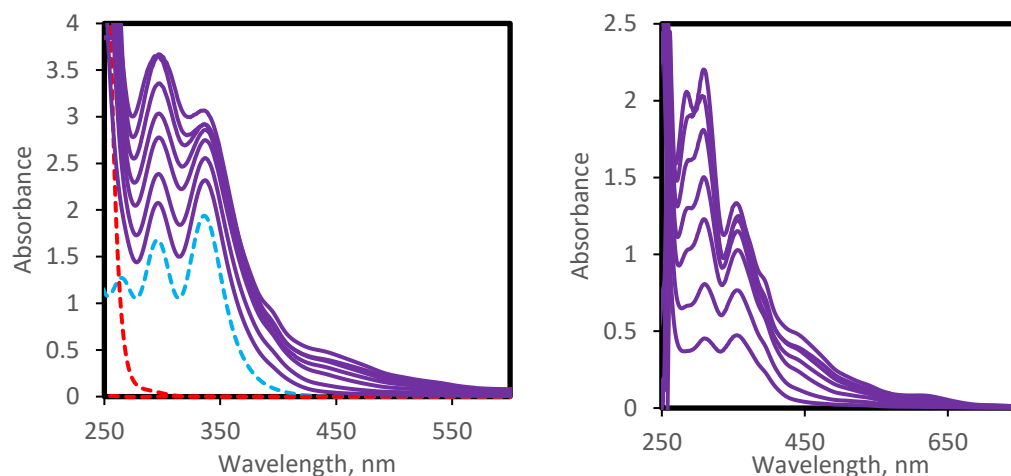


Figure S4. (Left) Spectra of the solutions with constant concentration of CHI_3 and various concentrations of triethylamine (TEA). Spectra of the solutions of individual reactants are shown as dashed blue (CHI_3) or red (TEA) lines. (Right): Spectra of the complexes obtained by subtraction of the absorption of components from the spectra of their mixtures

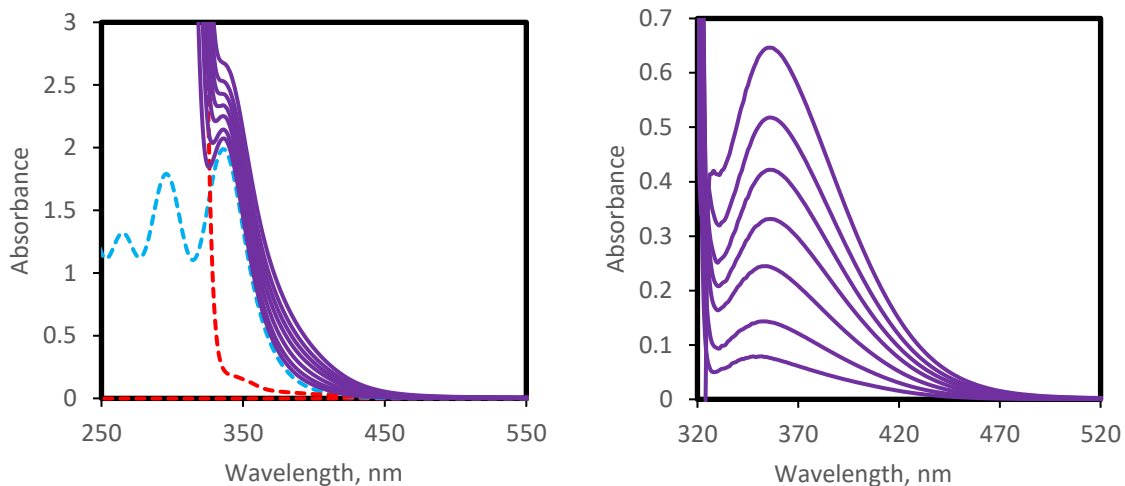


Figure S5. (Left) Spectra of the solutions with constant concentration of CHI_3 and various concentrations of m-methoxy-N,N-dimethylaniline (mMeODMA). Spectra of the solutions of individual reactants are shown as dashed blue (CHI_3) or red (mMeODMA) lines. (Right): Spectra of the complexes obtained by subtraction of the absorption of components from the spectra of their mixtures

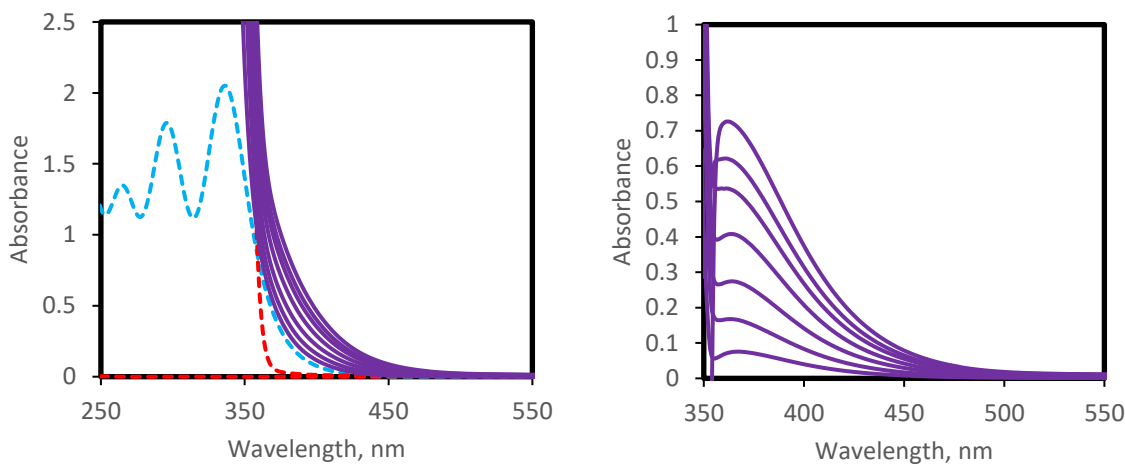


Figure S6. (Left) Spectra of the solutions with constant concentrations of CHI_3 and various concentrations of p-methoxy-N,N-dimethylaniline (pMeODMA). The spectra of the solutions of the individual reactants are shown as dashed blue (CHI_3) or red (pMeODMA) lines. (Right): Spectra of the complexes obtained by subtraction of the absorption of components from the spectra of their mixtures

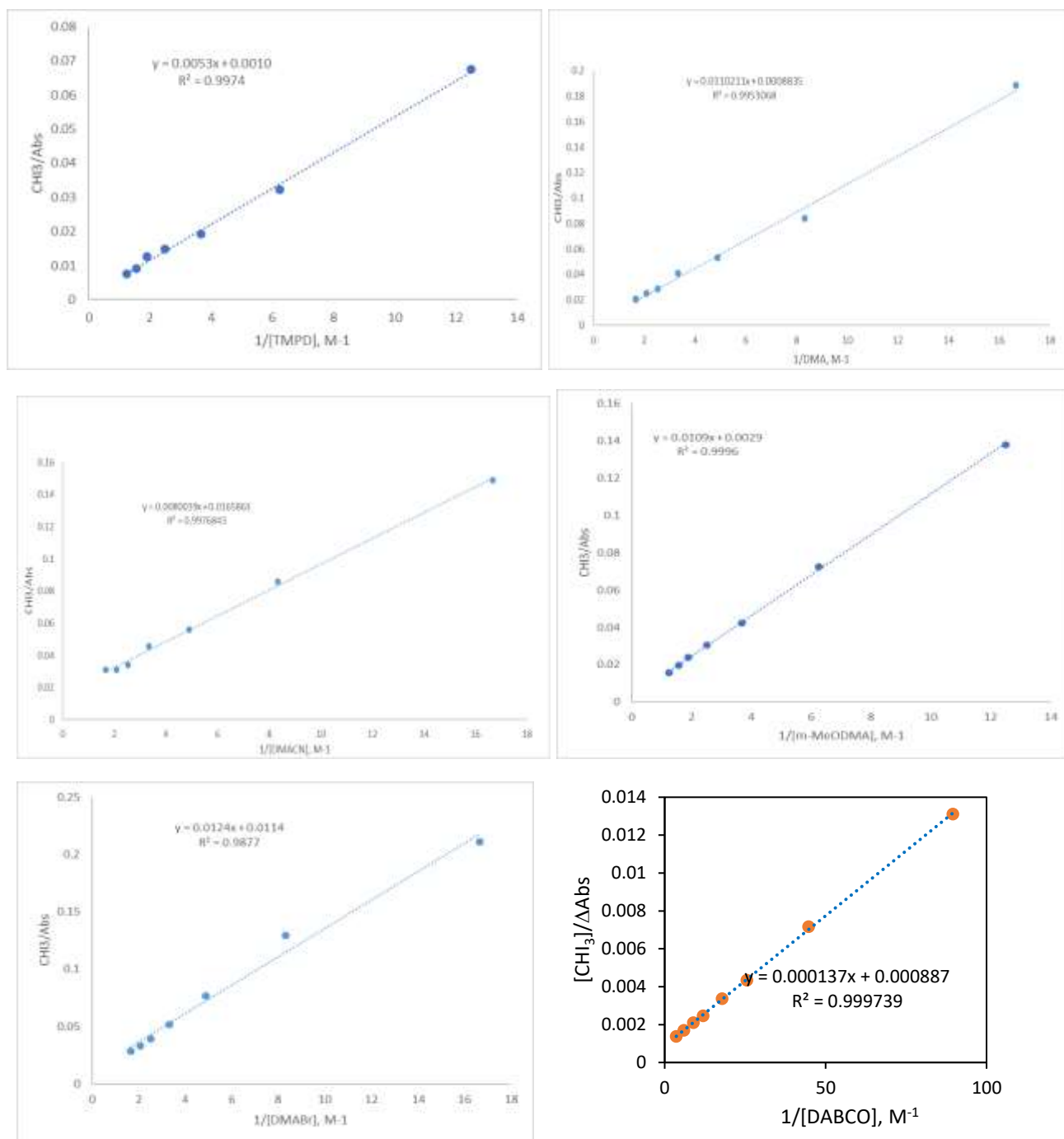


Figure S7. Benesi-Hildebrand plots based on the UV-Vis spectra of solutions of CHI₃ with amines.

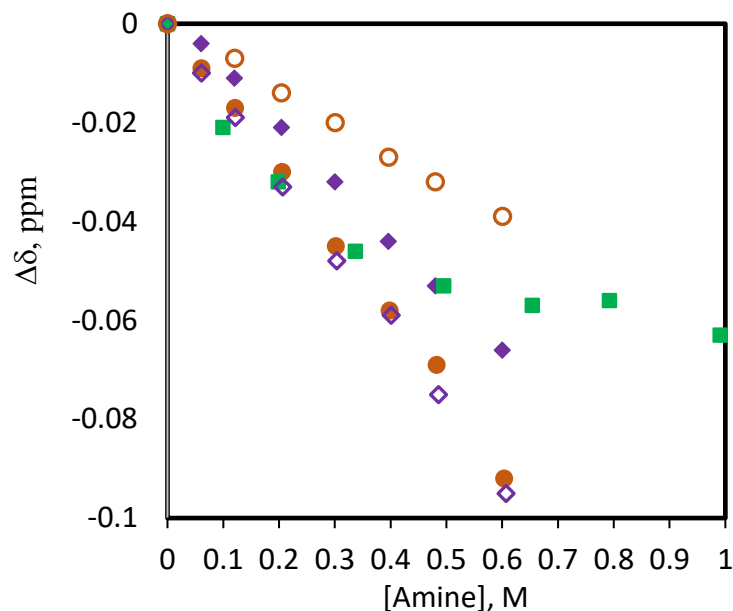


Figure S8. Dependencies of the chemical shifts of the protons of CHI_3 (as compared to that in the corresponding isolated molecules) on the concentration of added trimethylamine (TEA) (■), DMA (●), DMACN (○), DMABr (◆) or mMeODMA (◇) (in CD_3CN , 22°C).

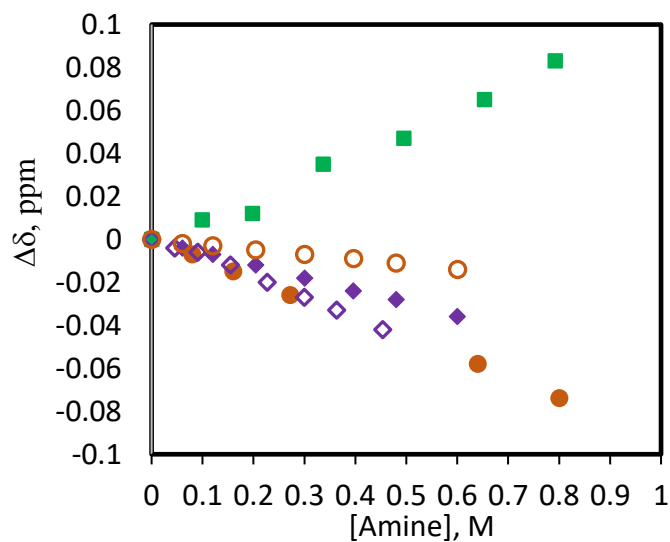


Figure S9. Dependencies of the chemical shifts of the protons of CHBr_3 (as compared to that in the corresponding isolated molecules) on the concentration of added TEA (■), DMA (●), DMACN (○), DMABr (◆) or mMeODMA (◇) (in CD_3CN , 22°C).

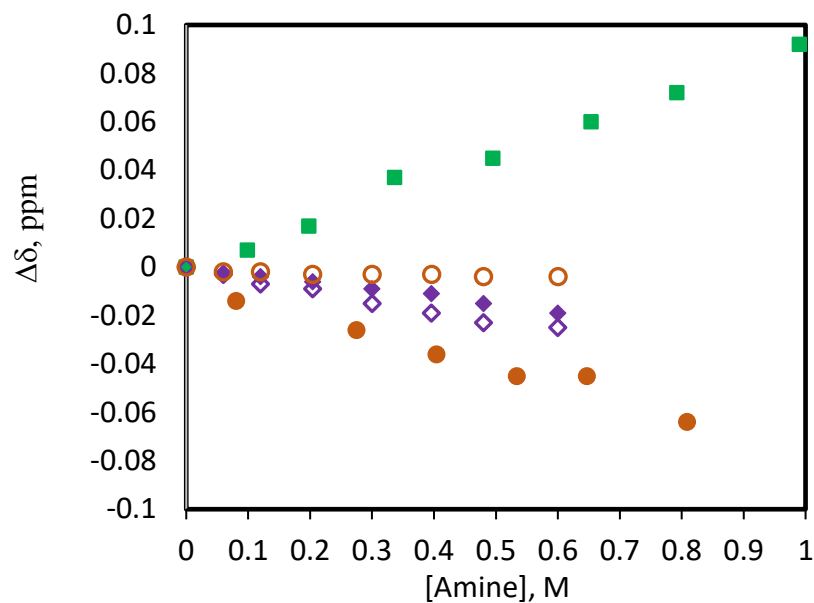


Figure S10. Dependencies of the chemical shifts of the protons of CHCl_3 as compared to that in the corresponding isolated molecules) on the concentration of added TEA (■), DMA (●), DMACN (○), DMABr (◆) or mMeODMA (◇) (in CD_3CN , 22°C).

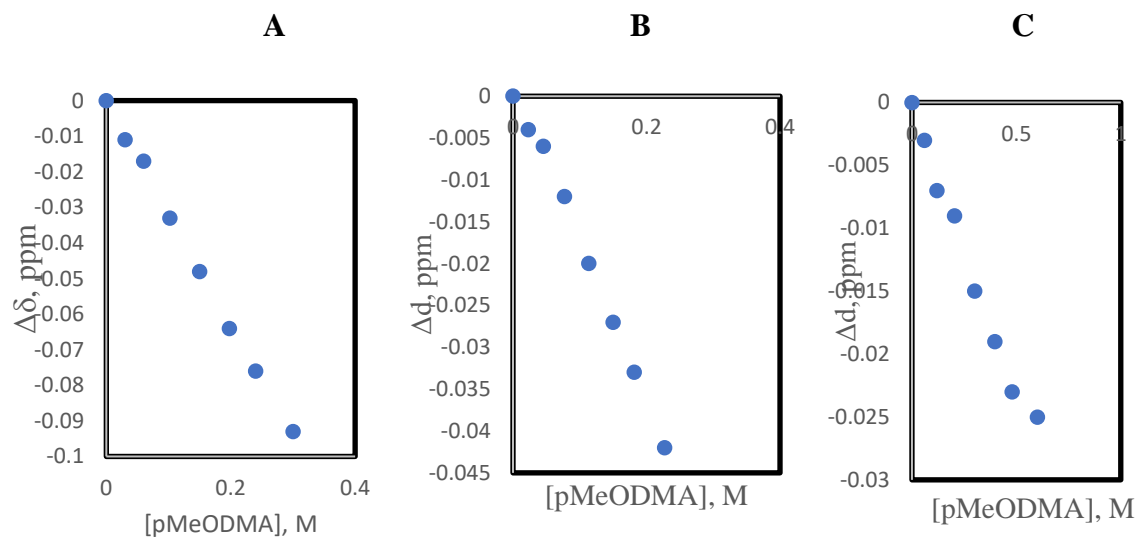


Figure S11. ^1H NMR shifts occurring upon the addition of pMeODMA to solutions containing CHI_3 (A), CHBr_3 (B), and CHCl_3 (C).

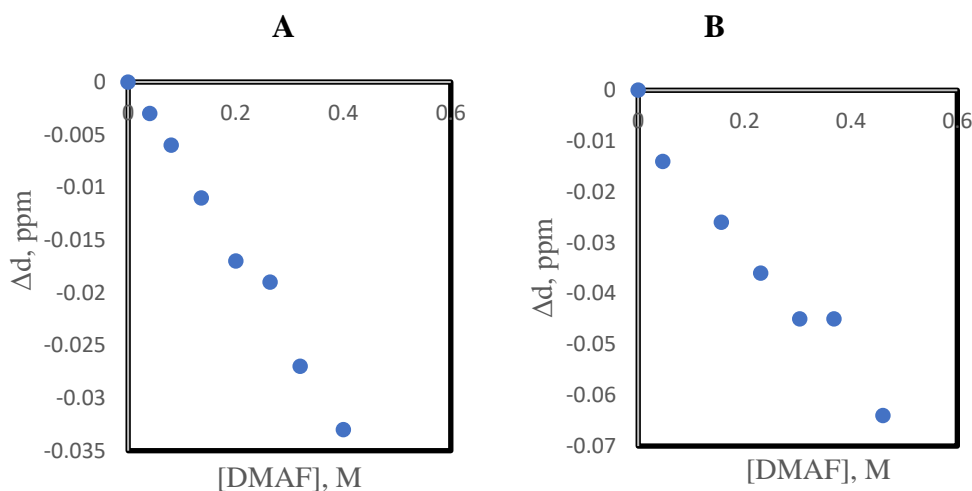


Figure S12. ^1H NMR shifts occurring upon the addition of DMAF to solutions CHBr_3 (A), and CHCl_3 (B).

Table S1: Energies of HyB and HaB complexes between CHX_3 and amines obtained from M06-2X/def-TZVPP computations (acetonitrile).

CHX ₃	Amine	Energy + ZPE, Hartree		BSSE, Hartree	
		HaB complex	HyB complex	HaB complex	HyB complex
CHI ₃	DABCO	-1276.702449	-1276.698772	0.000676	0.000626
	TMPD	-1431.471322	-1431.471276	0.000619	0.000635
	DMA	-1297.587684	-1297.58828	0.0004994	0.0005746
	DMAF	-1396.847931	-1396.847962	0.0005648	0.0005887
	DMACN	-1389.847013	-1389.848308	0.00045929	0.0004862
	p-MeODMA	-1412.07885	-1412.080087	0.00042381	0.0005791
	DMABr	-3871.195498	-3871.195937	0.00051254	0.0005571
	m-MeODMA	-1412.083703	-1412.085067	0.00052216	0.0006268
CHBr ₃	DABCO	-8106.386286	-8106.387885	0.000667	0.000793
	TMPD	-8261.157135	-8261.159697	0.000649	0.000902
	DMA	-8127.274722	-8127.276463	0.0005746	0.0005532
	DMAF	-8226.535234	-8226.53654	0.0005694	0.000856
	DMACN	-8219.535116	-8219.536826	0.00051866	0.0007535
	p-MeODMA	-8241.767342	-8241.76941	0.00059426	0.0008173
	DMABr	-10700.88272	-10700.88507	0.00055527	0.0008149
CHCl ₃	DABCO	-1764.400973	-1764.404661	0.000553	0.000832
	TMPD	-1919.172264	-1919.176305	0.000583	0.00094
	DMA	-1785.290752	-1785.293591	-1785.29075	0.00083708
	DMAF	-1884.551226	-1884.553148	-1884.55123	0.00085602
	DMACN	-1877.551723	-1877.554029	-1877.55172	0.00084004
	p-MeODMA	-1899.782331	-1899.786337	-1899.78233	0.00056352
	DMABr	-4358.898963	-4358.901941	-4358.89896	0.00085528
	m-MeODMA	-1899.786913	-1899.789983	-1899.78691	0.00092482

Table S2: Energies of individual CHX₃ and amines obtained from M06-2X/def-TZVPP computations (acetonitrile).

Amines	Energy+ZPE, Hartree	CHX ₃	Energy+ZPE, Hartree
TMPD	-499.897003	CHI ₃	-931.564856
DABCO	-345.125783	CHBr ₃	-7761.254232
DMA	-366.015030	CHCl ₃	-1419.271718
DMAF	-465.275445		
DMACN	-458.276480		
DMABr	-2939.623390		
pMeODMA	-480.507145		
mMeODMA	-480.511176		

Table S3. Electron densities and energies ($\rho(r)$ and $H(r)$, in a.u.) at BCPs along HaB and HyB bond paths.

Amines	HaB complexes		HyB complexes	
	$\rho(r)\times 10^2$	$H(r)\times 10^3$	$\rho(r)\times 10^2$	$H(r)\times 10^3$
CHI ₃				
DMA	2.13	0.07	1.36	1.40
DMAF	2.39	-0.42	2.05	0.57
DMABr	2.02	0.25	1.41	1.25
DMACN	1.68	0.72	1.27	1.29
mMeODMA	2.11	0.11	1.47	1.37
pMeODMA	1.04	0.92	1.31	1.41
CHBr ₃				
DMAF	2.36	0.48	2.03	0.58
DMABr	1.65	1.15	1.07	1.41
DMACN	1.41	1.29	1.25	1.29
mMeODMA	1.70	1.12	1.57	1.12
pMeODMA	1.87	0.96	1.71	0.98
CHCl ₃				
DMA	1.45	1.66	1.21	1.42
DMAF	1.49	1.63	1.89	0.82
DMABr	1.39	1.69	1.05	1.40
DMACN	1.19	1.75	0.58	1.19
mMeODMA	1.43	1.67	1.46	1.25
pMeODMA	1.62	1.53	1.30	1.43

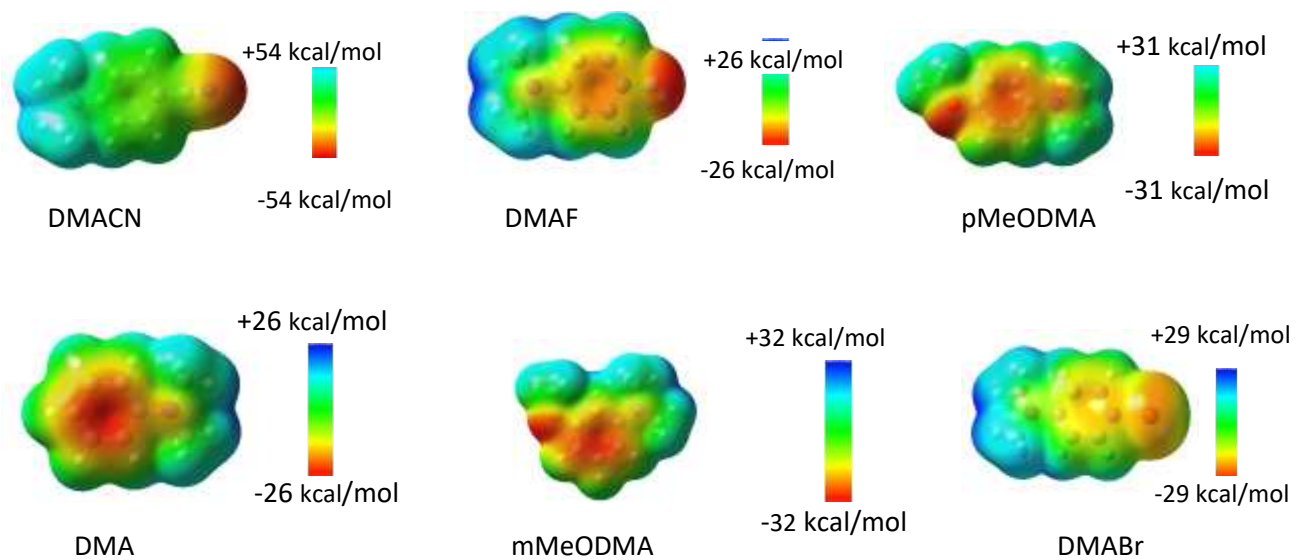


Figure S13. Electrostatic potential (calculated at 0.001 electrons Bohr⁻³ electronic density) on the molecular surfaces of other aromatic amines.

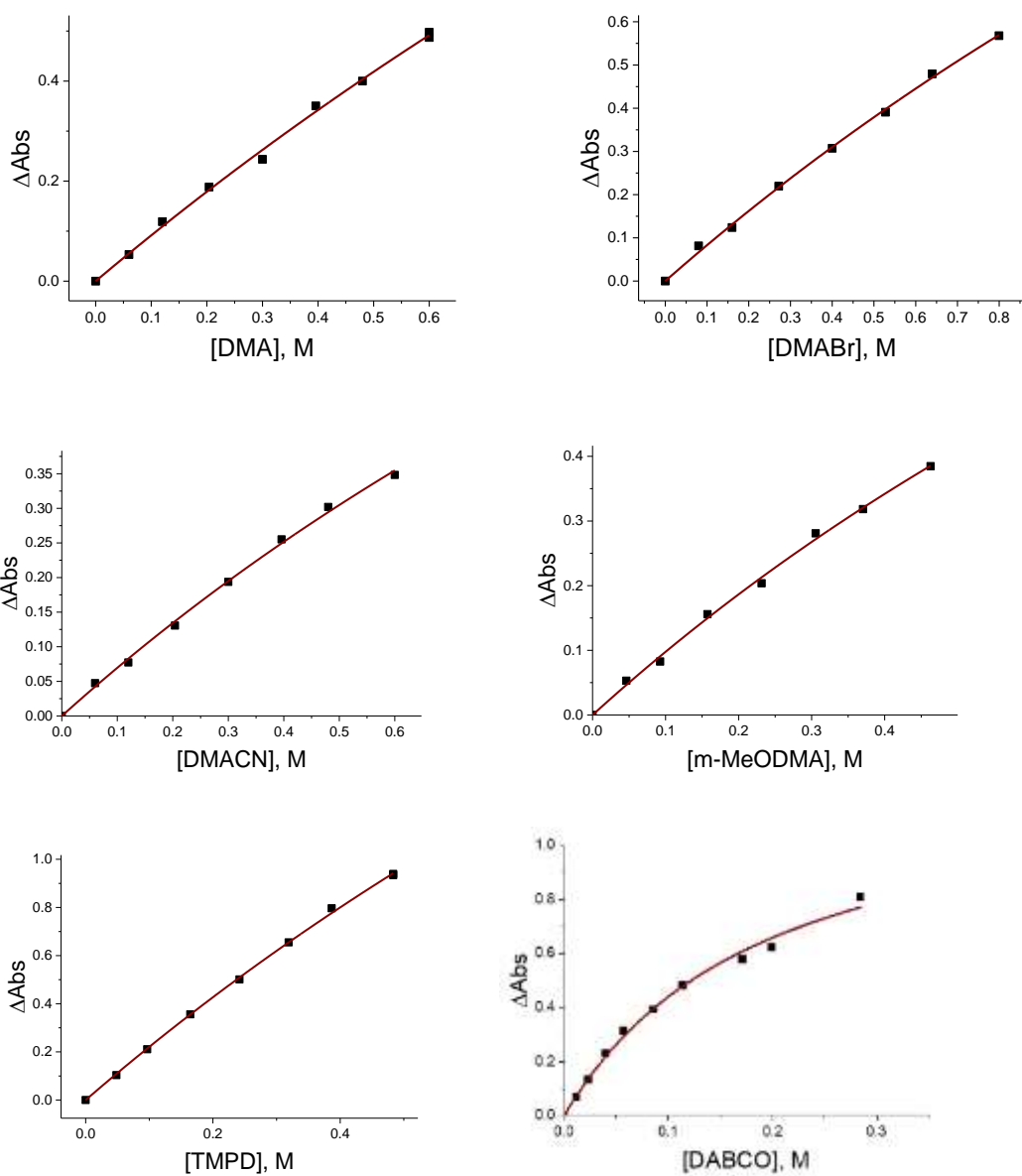


Figure S14. Dependencies of the ΔAbs and $\Delta\delta$ values in the solutions with a constant concentration of CHI_3 (0.01 M) and variable aliphatic and aromatic amine concentrations. The solid lines show the simultaneous multivariable fitting of the UV-Vis and NMR titration data.

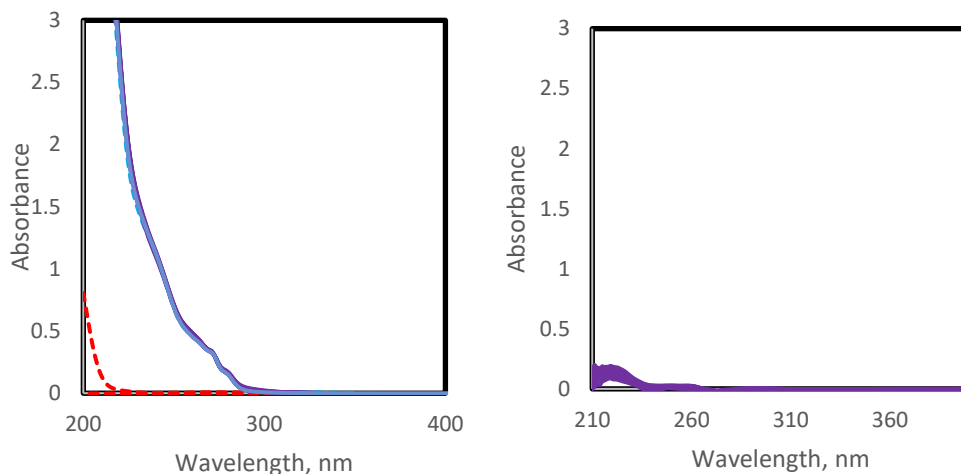


Figure S15: (Left) Spectra of solutions with constant concentrations of H-Im-iPrArI (0.4mM) and various concentrations of tetrabutylammonium iodide (TBACl). The spectra of the solutions of the individual reactants are shown by dashed blue (H-Im-iPrArI) and red (TBACl) lines. (Right) Spectra of the complexes obtained by subtracting the absorption of components from the spectra of their mixtures.

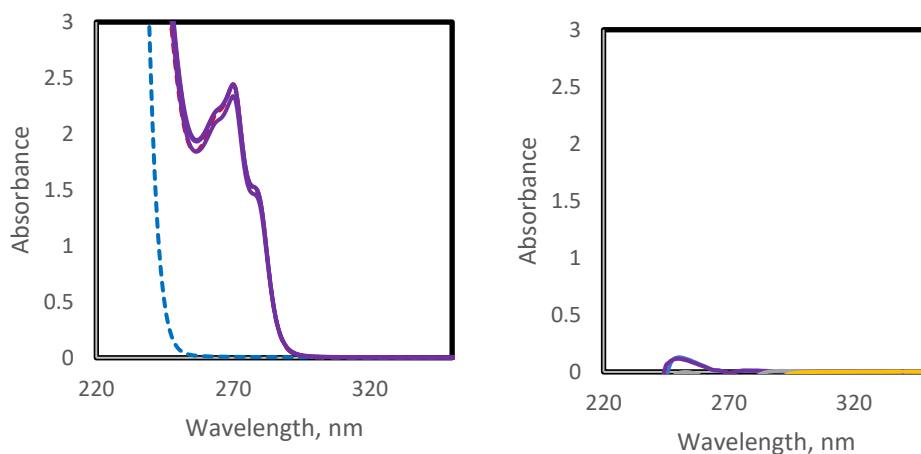


Figure 16. (Left) Spectra of solutions with constant concentrations of H-Im-iPrArH (0.4mM) and various concentrations of tetrabutylammonium iodide (TBABr). The spectra of the solutions of the individual reactants are shown by dashed blue (H-Im-iPrArH) and red (TBABr) lines. (Right) Spectra of the complexes obtained by subtracting the absorption of components from the spectra of their mixtures.

Table S4: Energies and UV-Vis values of HyB and HaB complexes between (halo)imidazolium and halides

Complexes	E w/zpe, hatree	zpe, hatree	E+zpe, hatree	ΔE, hatree
H-ImAr-I---I-	-1755.307358	0.576265	-1754.731093	-1757.616365
H-ImAr-I---Cl-	-1917.864567	0.576307	-1917.288260	-1920.180851
H-ImAr-I---Br-	-4031.868131	0.576174	-4031.291957	-4034.180025
H-ImAr-H---I-	-1458.279294	0.587943	-1457.691351	-1460.787923
H-ImAr-H---Cl-	-1620.836077	0.588077	-1620.248000	-1623.351891
H-ImAr-H---Br-	-3734.83988	0.587705	-3734.252175	-3737.351543
Cl-ImAr-I---I-	-2674.494163	0.557271	-2673.936892	-2676.614294
Cl-ImAr-I---Cl-	-2837.051975	0.557462	-2836.494513	-2839.179234
Cl-ImAr-I---Br-	-4951.055189	0.557376	-4950.497813	-4953.178011

Imidazoles	E of D w/zpe, hatree	zpe of D, hatree	E+zpe, hatree	UV	ϵ, $M^{-1} cm^{-1}$
H-ImArI	-1457.475850	0.576248	-1456.899602	215.16	10800
H-ImArH	-1160.449335	0.587448	-1159.861887	186.06	63000
Cl-ImAr-I	-2376.660550	0.556908	-2376.103642	232	11,800

Halides	E of X- w/zpe	E+zpe, hatree
I-	-297.818415	-297.818415
Br-	-2574.37678	-2574.37678
Cl-	-460.370291	-460.370291

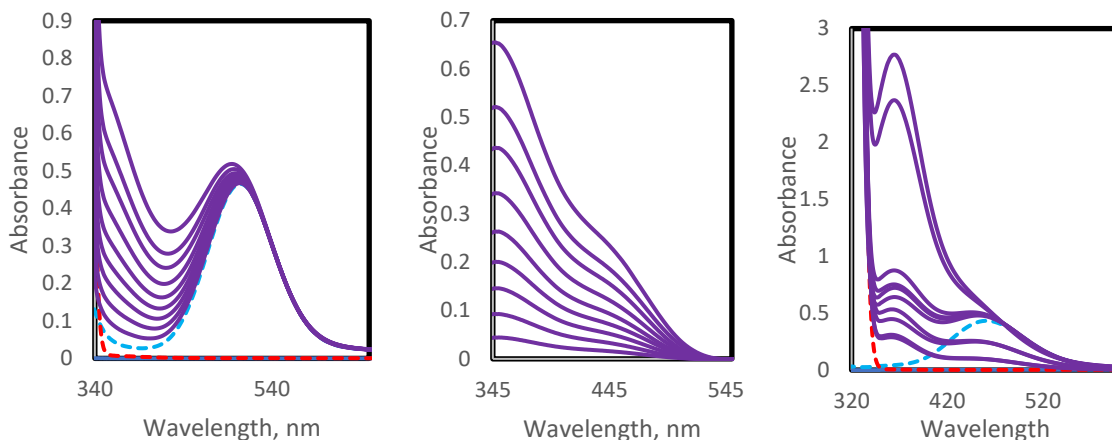


Figure S17. (Left) Spectra of the solutions with constant concentrations of I_2 and various concentrations of DMACN in DCM. The Spectra of the solutions of the individual reactants are shown as dashed blue (I_2) or red (DMACN) lines. (Centre) Spectra of the complexes obtained by subtracting the absorption of components from the spectra of their mixtures in DCM. (Right)- Spectra of the solutions with constant concentrations of I_2 and various concentrations of DMACN in AN.

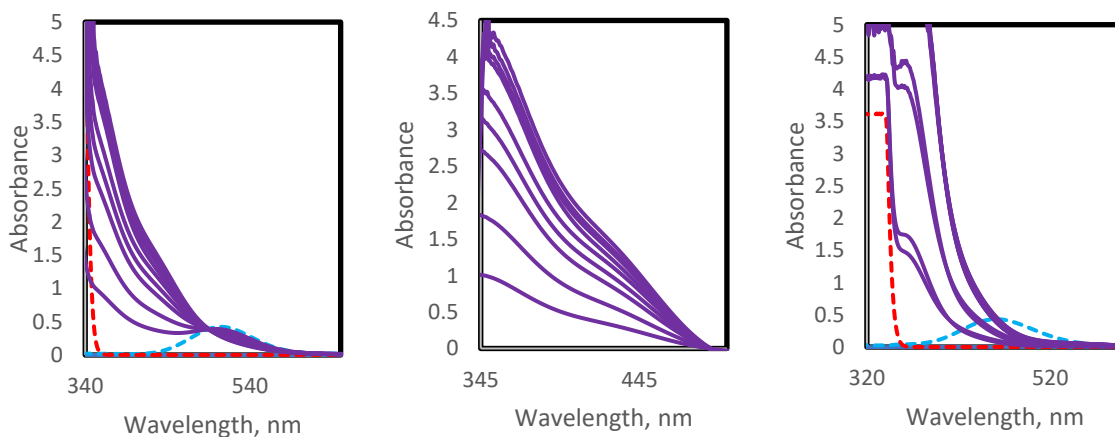


Figure S18. (Left) Spectra of the solutions with constant concentrations of I_2 and various concentrations of DMAF in DCM. The Spectra of the solutions of the individual reactants are shown as dashed blue (I_2) or red (DMAF) lines. (Centre) Spectra of the complexes obtained by subtracting the absorption of components from the spectra of their mixtures in DCM. (Right)- Spectra of the solutions with constant concentrations of I_2 and various concentrations of DMAF in AN.

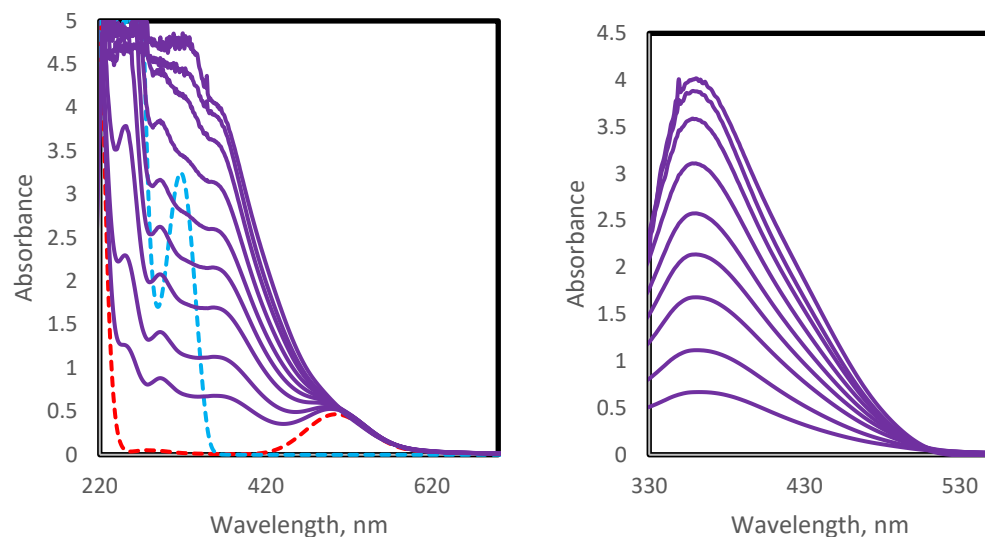


Figure S19. (Left) Spectra of solutions with constant concentration of I₂ and various concentrations of pMeODMA. The Spectra of the solutions of the individual reactants are shown as dashed blue (I₂) or red (pMeODMA) lines. (Right) Spectra of the complexes obtained by subtracting the absorption of components from the spectra of their mixtures.

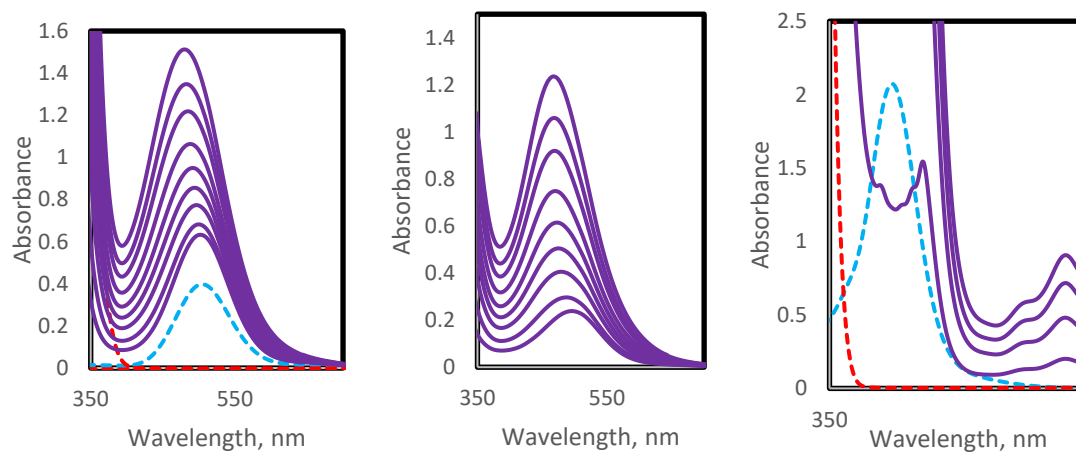


Figure S20. (Left) Spectra of solutions with constant concentration of I₂ and various concentrations of MPTZ. The individual reactants are shown as dashed blue (I₂) or red (MPTZ) lines. (Center) Spectra of the complexes obtained by subtracting the absorption of components from the spectra of their mixtures. (Right) Spectra of the solutions with constant concentrations of I₂ and various concentrations of MPTZ in AN.

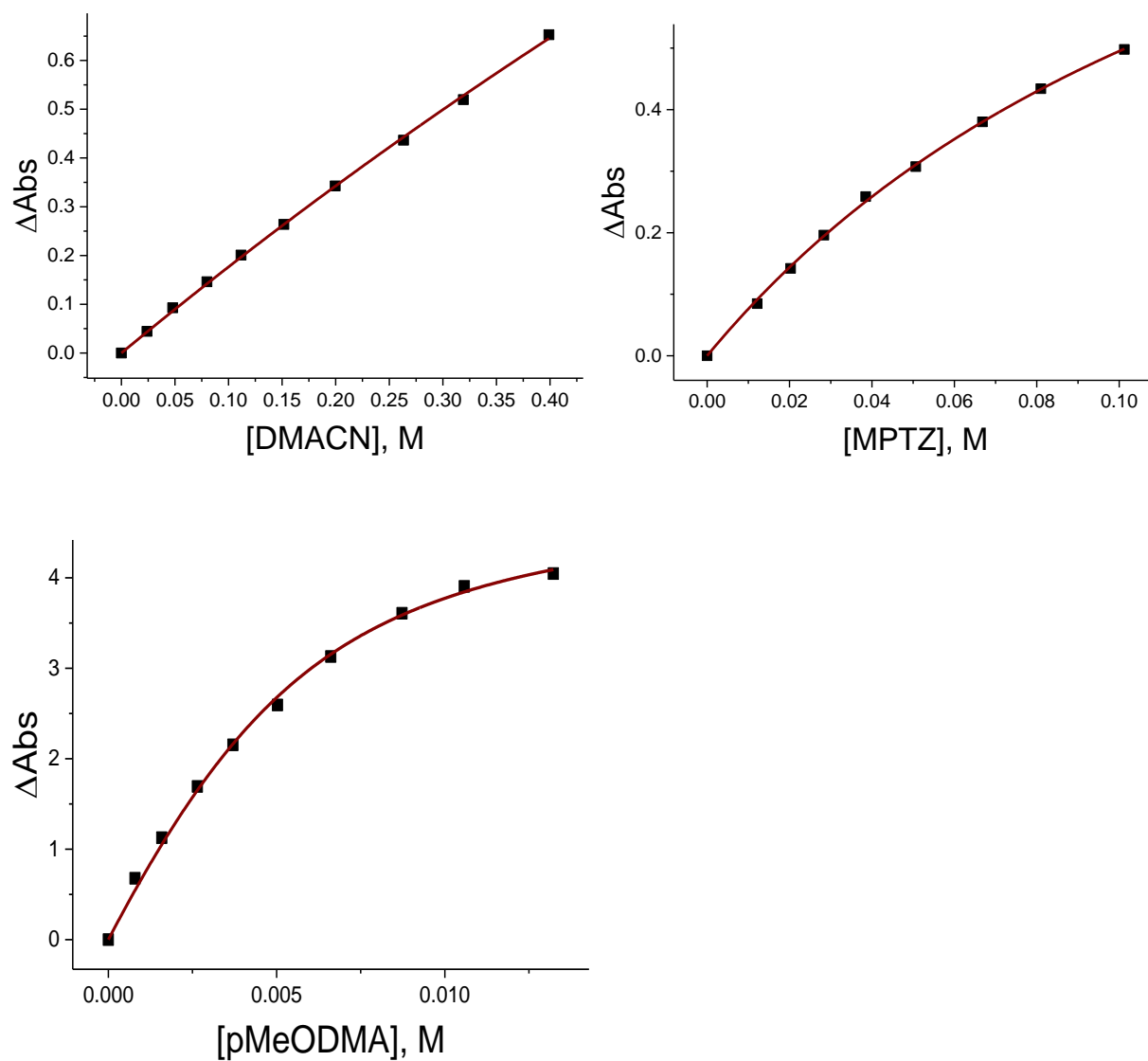


Figure S21. Dependencies of the ΔAbs and $\Delta\delta$ values in the solutions with a constant concentration of I_2 and variable aliphatic and aromatic amine concentrations.

Table S5: Energies of HaB complexes between molecular iodine with amines and some heterocyclic compounds in DCM, Acetonitrile, and Vacuum.

Amines	DCM			
	E w/zpe, hatree	zpe, hatree	E+zpe, hatree	BSSE, hatree
DMA	-961.4844216	0.177406	-961.3070156	0.001110
DMABr	-3535.080928	0.167122	-3534.913806	0.001094
DMACN	-1053.738201	0.175736	-1053.562465	0.001018
DMAF	-1060.736867	0.169144	-1060.567723	0.001120
pMeODMA	-1076.011749	0.210477	-1075.801272	0.001151
mMeODMA	-1076.013116	0.210393	-1075.802723	0.001133
TMPD	-1095.444095	0.251050	-1095.19304535	0.000910
MPTZ	-1550.218446	0.210045	-1550.00840149	0.001017
PTZ	-1510.921037	0.181374	-1510.73966294	0.001022
AN				
DMA	-961.4857225	0.177472	-961.3082505	0.001118
DMABr	-3535.082236	0.167208	-3534.915028	0.001102
DMACN	-1053.739921	0.175730	-1053.564191	0.001023
DMAF	-1060.738206	0.169197	-1060.569009	0.001126
pMeODMA	-1076.013663	0.210487	-1075.803176	0.001145
mMeODMA	-1076.014573	0.210407	-1075.804166	0.001138
TMPD	-1095.445753	0.251084	-1095.194669	0.001165
MPTZ	-1550.219646	0.210114	-1550.009532	0.000930
PTZ	-1510.922619	0.181417	-1510.741202	0.001022
Vacuum				
DMA	-961.4774802	0.177075	-961.3004052	0.001087
DMABr	-3535.073713	0.166769	-3534.906944	0.001054
DMACN	-1053.727153	0.175578	-1053.551575	0.000969
DMAF	-1060.729437	0.168776	-1060.560661	0.001077
pMeODMA	-1076.003376	0.210044	-1075.793332	0.001099
mMeODMA	-1076.005176	0.210131	-1075.795045	0.001084
TMPD	-1095.435144	0.250703	-1095.184441	0.000909
MPTZ	-1550.213410	0.209676	-1550.003734	0.000874
PTZ	-1510.912592	0.181300	-1510.731292	0.000994